

# Structure-Based Design of Ultrapotent Tricyclic Ligands for FK506-Binding Proteins

Patryk Krajczyk,<sup>[a]</sup> Christian Meyners,<sup>[a]</sup> Maximilian L. Repity,<sup>[a]</sup> and Felix Hausch\*<sup>[a, b]</sup>

Access to small, rigid, and sp<sup>3</sup>-rich molecules is a major limitation in the drug discovery for challenging protein targets. FK506-binding proteins hold high potential as drug targets or enablers of molecular glues but are fastidious in the chemotypes accepted as ligands. We here report an enantioselective synthesis of a highly rigidified pipecolate-mimicking tricyclic scaffold that precisely positions functional groups for interact-

ing with FKBP. This was enabled by a 14-step gram-scale synthesis featuring anodic oxidation, stereospecific vinylation, and *N*-acyl iminium cyclization. Structure-based optimization resulted in the discovery of FKBP inhibitors with picomolar biochemical and subnanomolar cellular activity that represent the most potent FKBP ligands known to date.

The precise tailoring of small molecules that perfectly match the binding pockets of proteins is at the core of drug discovery and a key activity of medicinal chemistry. A current trend to address increasingly challenging drug targets is to design novel scaffolds decorated with unusual chemotypes, which is reflected by a constant rise of molecular complexity.<sup>[1]</sup> This results in structures with lower aromatic ring count and higher sp<sup>3</sup> ratios.<sup>[2]</sup> It also emphasizes the importance of new synthetic methodologies and ability to introduce non-classical sp<sup>3</sup>-enriched isosteres that further extend the three-dimensional way of thinking.<sup>[2,3]</sup> Structural rigidification of a flexible ligand is a commonly used strategy during the lead optimization stage, which further contributes to the need for sp<sup>3</sup>-rich molecules.<sup>[4–6]</sup> Conformational preorganization can enhance binding affinity to a given biological target by minimizing the entropic penalty associated with the ligand adopting the bioactive conformation. Moreover, conformational restriction can improve selectivity, physicochemical properties, and metabolic stability.<sup>[7]</sup>

FK506-binding proteins belong to the immunophilin family that upon binding to clinically approved natural products FK506 and Rapamycin enable an immunosuppressive effect.<sup>[8]</sup> Among human FKBP, the Hsp90-associated co-chaperone FKBP51 contributes to the steroid hormone receptor maturation and plays a prominent role in human stress biology suggesting that FKBP51 inhibition has a therapeutic potential.<sup>[9–11]</sup> Starting

from FK506, we previously explored various series of pipecolate analogues as non-immunosuppressive FKBP inhibitors. This cumulated in the [4.3.1]aza-amide bicyclic core, which consistently shows improved binding properties in comparison to more flexible structures.<sup>[12–15]</sup> Due to the enhanced affinity these compounds were used in a broad spectrum of application including ligand-protein interaction studies,<sup>[16]</sup> development of selective proteolysis targeting chimeras (PROTACs),<sup>[17]</sup> molecular glues<sup>[18]</sup> and as anti-microbial agents.<sup>[19,20]</sup>

Encouraged by the strong positive impact of a single, solvent-exposed methyl group observed for [4.3.1]aza-amide bicyclic inhibitors<sup>[21]</sup> (Figure 1) we envisioned a new scaffold with an additional carbon bridge leading to a tricyclic system.<sup>[22]</sup> Analysis of previously obtained X-ray cocrystal structures of

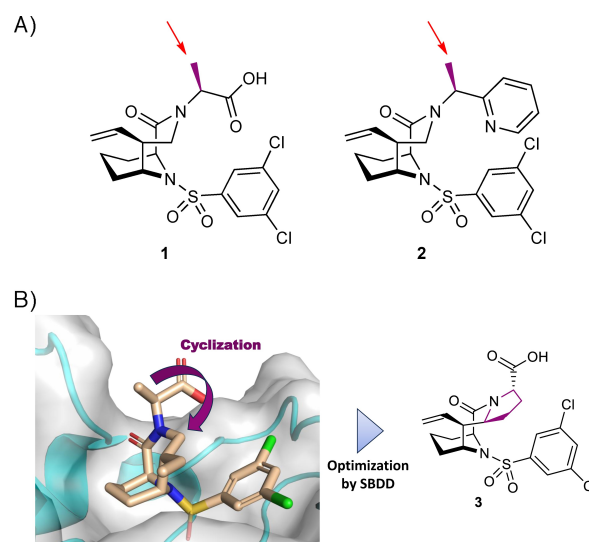


**Figure 1.** A) Chemical structures of high affinity bicyclic ligands 1 and 2 (known as compound 1<sup>(S)-Me</sup> and 16<sup>(S)-Me</sup> in ref. [21]), and B) their tricyclic analogue 3 explored in this work (additional bridge highlighted in purple). The affinity-boosting methyl groups in the  $\alpha$ -position of 1 and 2 are indicated by red arrows. The cyclization approach is marked with purple, curved arrow. Cocrystal structures of 1 (pale orange sticks) in complex with FKBP51 (grey surface with cyan cartoon, PDB: 7APS). The side chains of Phe<sup>77</sup>, Glu<sup>75</sup> and Arg<sup>73</sup> have been omitted for clarity.

[a] P. Krajczyk, C. Meyners, M. L. Repity, F. Hausch  
Institute for Organic Chemistry and Biochemistry, Technical University  
Darmstadt, Peter-Grünberg-Straße 4, Darmstadt 64287, Germany  
E-mail: felix.hausch@tu-darmstadt.de

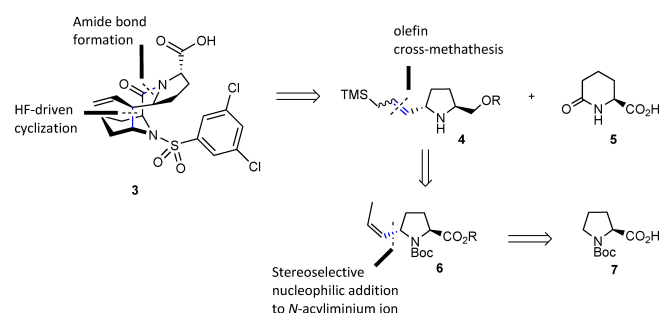
[b] F. Hausch  
Centre for Synthetic Biology, Technical University of Darmstadt, Darmstadt  
64283, Germany

Supporting information for this article is available on the WWW under  
<https://doi.org/10.1002/chem.202401405>

© 2024 The Authors. Chemistry - A European Journal published by Wiley-VCH  
GmbH. This is an open access article under the terms of the Creative  
Commons Attribution Non-Commercial License, which permits use, dis-  
tribution and reproduction in any medium, provided the original work is  
properly cited and is not used for commercial purposes.

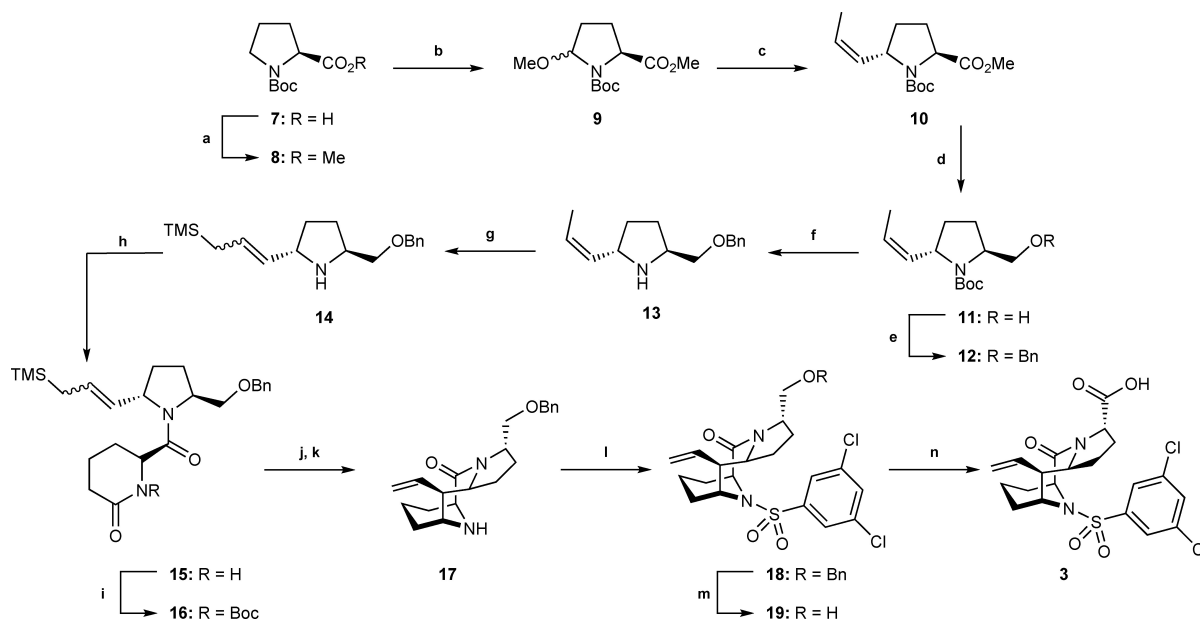
compounds **1** and **2** bound to FKBP51 suggested that elongation of the methyl group in the C- $\alpha$ -position could form a cyclized, rigidified product with defined geometry. This product was predicted to retain a conformation compatible with the binding mode of known FKBP ligands. To maximize the contribution of proposed structural changes we provided a new exit vector in the form of a functional group amenable to the common medicinal chemistry transformations.

To reduce this to practice, we report here an enantioselective synthesis of the envisioned novel,  $sp^3$ -enriched tricyclic scaffold and a series of structurally optimized compounds. Retrosynthetic analysis (Scheme 1) based on HF-driven (*N*-acyliminium) cyclization and amide bond formation suggested building block **4** as the key intermediate. Compound **4** could be accessible via cross metathesis from *trans*-5-propenylproline building block **6**, which was envisioned to be synthesized stereoselectively from the amino acid **7** as chiral starting material.



**Scheme 1.** Retrosynthetic analysis of **3** based on HF-driven cyclization.

The synthesis began by methylation of *N*-*tert*-butoxycarbonyl (Boc-) protected *L*-proline **7** to give methyl ester **8** in 90% yield<sup>[23]</sup> (Scheme 2). In order to functionalize the proline ring at the C5 position, the carbamate was subjected to Shono-type anodic oxidation using graphite electrodes (6.3×150 mm, 250 mA) and a 0.05 M solution of Et<sub>4</sub>NOTs in methanol as a supporting electrolyte.<sup>[24]</sup> This uncomplicated transformation could be run on a multigram scale in an open beaker. After 5.0 F/mol has passed the methoxylated product **9** was obtained in 88% yield as a 1:1 mixture of diastereoisomers. The transformation to the key 2,5-disubstituted pyrrolidine derivative **10** was accomplished in 76% yield through BF<sub>3</sub>Et<sub>2</sub>O-mediated reaction with the vinyl cuprate prepared in situ from *trans*-1-bromopropene.<sup>[25]</sup> The stereochemistry of the obtained product was elucidated on the basis of correlations observed in the NOESY experiment after its conversion into the deprotected pyrrolidine derivative (see Supporting Information, Figure S1). Gratifyingly, the conditions employed for the nucleophilic addition to **9** preferentially yielded the *trans* adduct, which is essential for constructing the tricyclic core fragment with the desired stereochemistry. Ester reduction by LiBH<sub>4</sub> gave the primary alcohol **11** in 87% yield, which was further converted into benzyl derivative **12**. Deprotection of the Boc group with bromotrimethylsilane (TMSBr) provided *trans*-5-propenylproline benzyl ether **13** as a free amine in quantitative yield. However, a subsequent cross metathesis (CM) with allyltrimethylsilane turned out to be challenging, consistent with known poor suitability of amines as substrates for ruthenium-based olefin metathesis.<sup>[26]</sup> This is thought to be due to a possible coordination of the polar functional groups to the emerging carbene, spoiling catalytic activity. The use of titanium or

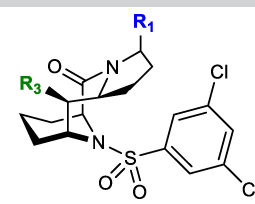
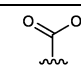
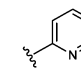
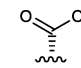
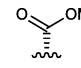
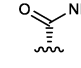
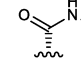
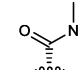
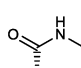
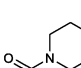
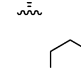
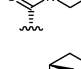
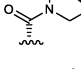
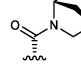
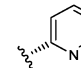
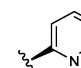
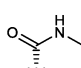


**Scheme 2.** Synthesis of the tricyclic ligand **3**. Reagents and conditions: (a) K<sub>2</sub>CO<sub>3</sub>, MeI, DMF, rt, 17 h, 90%; (b) graphite anode, Et<sub>4</sub>NOTs/MeOH, 250 mA, 5.0 F/mol, 5 °C, 88%; (c) (*Z*)-prop-1-en-1-yl lithium, CuBr·Me<sub>2</sub>S, BF<sub>3</sub>·Et<sub>2</sub>O, -78 °C to rt, 30 min, 76%; (d) LiBH<sub>4</sub>, THF, 0 °C to rt, 17 h, 87%; (e) NaH, benzyl bromide, THF, 0 °C to rt, 17 h, 81%; (f) TMSBr, DCM, rt, 17 h, quant.; (g) allyltrimethylsilane, Cy<sub>2</sub>BCl, Grubbs II, DCM, reflux, 3 h, 71%; (h) (*S*)-6-oxo-2-piperidinecarboxylic acid **5**, HATU, DIPEA, DMF, rt, 4 h, 56%; (i) Boc<sub>2</sub>O, DIPEA, DMAP, DCM, rt, 36 h, 88%; (j) DIBAL-H, THF, -78 °C, 15 min; (k) HF, DCM, -78 °C to 0 °C, 3 h, 65% (over 2 steps); (l) 3,5-dichlorobenzenesulfonyl chloride, DIPEA, MeCN, rt, 17 h, 68%; (m) BCl<sub>3</sub>·SMe<sub>2</sub>, DCM, rt, 1 h, 84%; (n) Jones reagent, acetone, 0 °C to rt, 2 h, 87%.

boron-based Lewis acids to improve olefin metathesis has been already reported.<sup>[27]</sup> In order to access the functionalized proline derivative via CM, various catalysts and Lewis acids additives were screened (see Supporting Information, Table S1 and S2). The combination of a 2<sup>nd</sup> generation Grubbs catalyst (7 mol%) and chlorodicyclohexyl borane (20 mol%) afforded the best results. Ultimately, the reaction performed in anhydrous DCM at reflux provided **14** in notable yield of 71%. With this compound in hand, we continued the synthesis to construct the tricyclic scaffold. Compound **14** was first coupled to commercially available (*S*)-6-oxo-2-piperidinecarboxylic acid **5** using HATU to deliver stereochemically pure amide **15** in 56% yield. Subsequent Boc protection resulted in **16** as a precursor for the key cyclization step. Chemoselective reduction with DIBAL-H and subsequent treatment of hydroxy carbamate with hydrofluoric acid in pyridine resulted in the target tricyclic building block **17** as the only diastereomer obtained in 65% yield over 2 steps.<sup>[15,19,21]</sup> Reaction with 3,5-dichlorosulfonyl chloride furnished sulfonamide **18**, which after treatment with boron trichloride methyl sulfide complex afforded alcohol **19**. Jones oxidation of primary alcohol provided the functionalized FKBP ligand **3** in excellent yield of 87% on a gram scale for testing and further derivatization. The presented synthetic route (Scheme 2) facilitated the gram-scale synthesis of tricyclic compound **3** with an overall yield of 5% over fourteen steps. In order to prepare 1 g of **3** nearly 12.5 g (58 mmol) of *N*-Boc-*L*-proline is needed. All synthetic steps employed were scaled to the gram quantities, and their products were purified via standard chromatographic methods.

To get a first glimpse on activity, **3** was tested for binding to purified human FKBP12 and FKBP51. Gratifyingly, **3** bound to the former with 12 nM and to the latter with 698 nM (Table 1), providing a first indication for the suitability of the tricyclic scaffold as FKBP ligand. Compared to the starting compound **1**,<sup>[21]</sup> this is almost identical for FKBP12 ( $K_i = 13$  nM for **1**) but substantially worse for FKBP51 ( $K_i = 22$  nM for **1**). Encouraged by this finding we investigated the molecular interaction network of our tricyclic ligand and its exact spatial architecture by determining the cocrystal structure of ligand **3** in complex with the FK1 domain of FKBP51 (Figure 2A). As intended, all key interactions of the original [4.3.1]sulfonamide motif are conserved, incl. van der Waals interactions with Trp<sup>90</sup>, Ile<sup>87</sup>, Val<sup>86</sup>, Phe<sup>77</sup>, Tyr<sup>57</sup>, a hydrogen bond to Ile<sup>87</sup>, non-canonical hydrogen bond-like interactions with the sulfonamide,<sup>[16]</sup> and a halogen bond to Ser<sup>118</sup>. The overlay with bicyclic ligand **1** bound to FKBP51 showed that both compounds bind in an almost identical pose (Figure 2B). The only substantial difference is the orientation of the carboxylic group, which for **1** is shifted by 36° in comparison to **3**. ( $C^1-N-C^2-C^3$  dihedral angle, see also Supporting Information). This is enforced by the geometry of the additional pyrrolidine ring. Notably, one oxygen of the carboxyl group remains hydrogen-bonded to Tyr<sup>113</sup> by a compensatory rotation of the  $N-C^2-C^3=O$  bond. In light of the newly identified spatial orientation of the carboxylic acid group in the cocrystal structure of the tricyclic scaffold, we explored the potential of substituents at this position. Towards this goal, the carboxylic acid was converted to its methyl ester **20** and to

**Table 1.** Overview of binding affinities of the tricyclic analogues **3–32** as well as bicyclic reference compounds **1** and **2**, obtained by a competitive fluorescence polarization assay.<sup>[31]</sup>

Entry	R1	R3	FKBP51 K <sub>i</sub> [nM]	FKBP12 K <sub>i</sub> [nM]
				
<b>1</b> <sup>[a,b]</sup>		vinyl	22	13
<b>2</b> <sup>[a,b]</sup>		vinyl	2.6	0.72
<b>3</b>		vinyl	698 ± 49	12 ± 1.7
<b>20</b>		vinyl	76 ± 10	1.0 ± 0.1
<b>21</b>		vinyl	18 ± 3.0	0.48 ± 0.08
<b>22</b>		vinyl	7.7 ± 0.9	0.32 ± 0.04
<b>23</b>		vinyl	121 ± 8.0	2.3 ± 0.2
<b>24</b>		vinyl	1.1 ± 0.4	0.043 ± 0.01
<b>25</b>		vinyl	0.93 ± 0.2	0.067 ± 0.01
<b>26</b>		vinyl	11 ± 0.7	0.16 ± 0.018
<b>27</b>		vinyl	17 ± 1.7	0.55 ± 0.07
<b>28</b>		vinyl	52 ± 6.0	0.72 ± 0.1
<b>(S)</b> - <b>30</b>		vinyl	464 ± 79	12 ± 1.6
<b>(R)</b> - <b>30</b>		vinyl	8990 ± 1000	558 ± 102
<b>31</b>		-CH <sub>2</sub> OH	0.76 ± 0.2	0.013 ± 0.004
<b>32</b>		-CH <sub>2</sub> OH	0.72 ± 0.2	0.019 ± 0.007

[a] Presented  $K_i$  values were taken from ref. [21]. [b] Presented residues represent analogous substituents in a [4.3.1]bicyclic context.

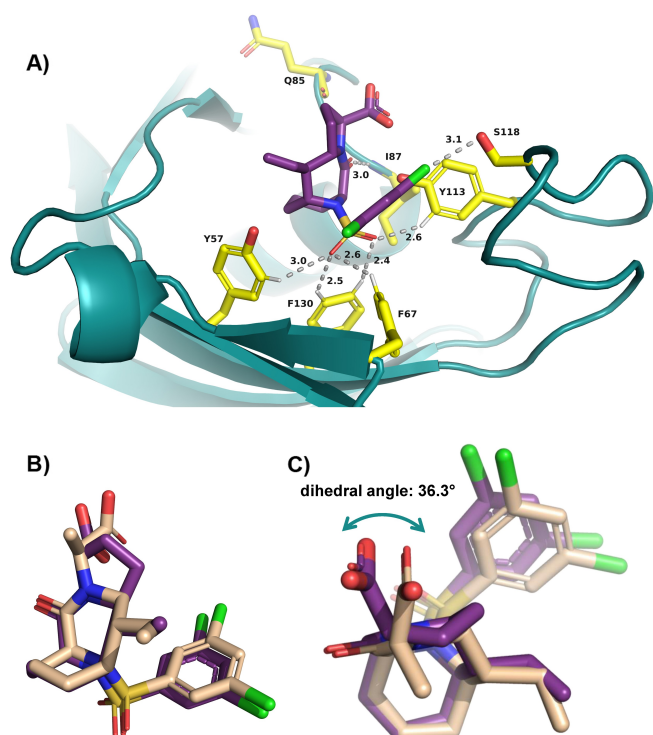
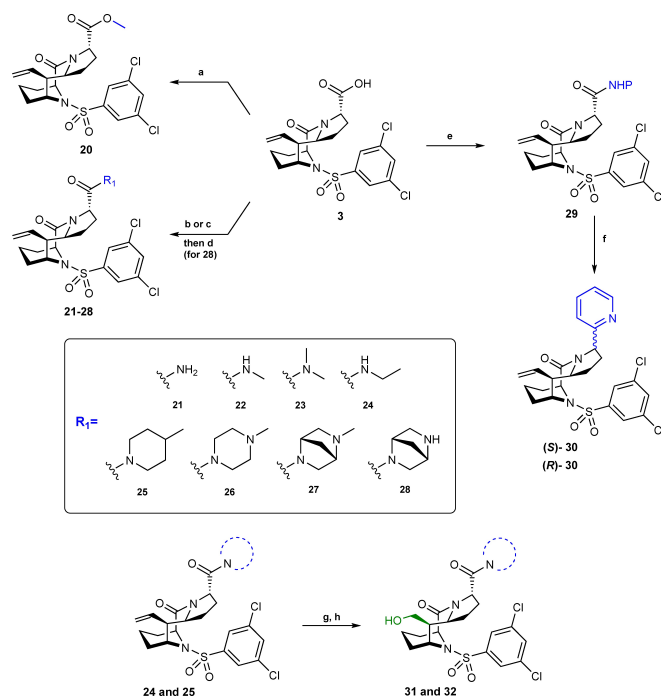


**Figure 2.** Molecular binding mode of **3** (PDB: 9EY3). A) The cocrystal structure of compound **3** (purple sticks) in complex with FKBP51 (cyan cartoon, key residues shown as yellow sticks). The main interactions with FKBP51 are indicated by dotted lines with the distances in Angstrom. Hydrophobic interactions with Trp<sup>80</sup>, Phe<sup>67</sup>, Val<sup>76</sup> are not shown. B) Superposition of compound **3** with bicyclic ligand **1** (pale orange, from PDB: 7APS). C) Comparison of dihedral angles (C<sup>1</sup>-N-C<sup>2</sup>-C<sup>3</sup>) between compound **1** and **3**. The dihedral angles were measured in PyMol.

the amides **21–28** (Scheme 3). Since pyridine (as in **2**, Figure 1) was one of the best carboxylic replacements for [4.3.1]bicyclic ligands – with better affinities for most FKBP5 – we were interested to explore this moiety also in the novel tricyclic context. We therefore referred to Ni-catalyzed decarboxylative cross-coupling, which has emerged as powerful transformation for the preparation of a diverse range of C–C bonds.<sup>[28]</sup> Starting from the *N*-hydroxyphthalimide (NHP) ester of **3**, compound **29** was successfully coupled with 2-iodopyridine in the presence of a NiCl<sub>2</sub>(bpy) as the pre-catalyst, chlorosilane additive and zinc reductant.<sup>[29,30]</sup> This provided two separable diastereomers (*S*)-**30** and (*R*)-**30**, which could be directly compared to the corresponding pyridine-based bicyclic ligands.<sup>[19,21]</sup> For two tricyclic analogues (**24** and **25**) we also explored the effect of converting the vinyl group to a hydroxyl group, as it tended to boost the binding affinities for bicyclic analogues. This was achieved by an oxidative cleavage followed by reduction.

The binding affinities of resulting tricycles **20–32** for human FKBP12 and FKBP51 were determined by a fluorescence polarization assay (Table 1).<sup>[31]</sup> Masking the negative charge of carboxylic acid as in **20** improved the affinity for both FKBP5 dramatically compared to the parent tricycle **3**. Unexpectedly, introduction of a heterocyclic pyridine ring as a carbonyl mimetic ((*S*)-**30**) did not improve affinity in the tricyclic context. However, we observed clear dependence of the stereochemistry



**Scheme 3.** Synthesis of the tricyclic analogues **20–32**. Reagents and conditions: (a) K<sub>2</sub>CO<sub>3</sub>, MeI, DMF, rt, 2 h, 94%; (b) CDI, NH<sub>3</sub> (30% in H<sub>2</sub>O), THF, rt, 30 min, quant. for **21**; (c) methylamine hydrochloride for **22**, dimethylamine for **23**, ethylamine for **24**, 4-methylpiperidine for **25**, 1-methylpiperazine for **26**, (1*R*,4*R*)-5-*t*-Boc-2,5-diazabicyclo-[2.2.1]heptane dihydrochloride for **27** or (1*S*,4*S*)-(-)-2-*t*-Boc-2,5-diazabicyclo[2.2.1]heptane for **28**, HATU, DIPEA, DMF, rt, 4–17 h, 78–95%; (d) TFA, DCM, rt, 1.5 h, quant.; (e) *N*-hydroxyphthalimide, EDC·HCl, DMAP, DCM, 0 °C to rt, 17 h, 97%; (f) 2-iodopyridine, NiCl<sub>2</sub>(bpy), TMSCl, Zn, DMA, rt, 3 h, 31%; (g) OsO<sub>4</sub>, NaIO<sub>4</sub>, 2,6-lutidine, dioxane/H<sub>2</sub>O (3:1), 0 °C to rt, 48 h; (h) NaBH<sub>4</sub>, EtOH, 0 °C to rt, 17 h, 78% for **31**, 76% for **32** (over 2 steps).

as the other diastereomer ((*R*)-**30**) bound substantially weaker. Surprisingly, the conversion to primary amide **21** provided a nearly 40-fold increase in potency for FKBP51 over compound **3**. Monomethylation of the amide as in **22** slightly improved affinity even further, while dimethylation as in **23** was counterproductive, suggesting the importance of a hydrogen bond donor. Indeed, the cocrystal structure of **21** confirmed a hydrogen bond to the carbonyl of Gln<sup>85</sup> (Figure 3), which was accompanied with a further rotational adaptation of the N–C<sup>2</sup>–C<sup>3</sup>(–O) dihedral angle. As observed for compound **3** before, all other interactions are virtually identical compared to the binding mode of **1**. To explore the scope of the amide substituents we elongated the alkyl group from methyl to ethyl as in tricycle **24**. Remarkably, this simple modification boosted affinity 7-fold for both FKBP5. Surprisingly, by expanding the *N,N*-dimethyl- to a 4-methyl piperidine motif, tricycle **25** displayed a dramatically increased affinity, binding 130-fold stronger to FKBP51 and 34-fold stronger to FKBP12 compared to the dimethylated analogue **23**.

However, introduction of an additional nitrogen as in compound **26** or in bridged diamines **27** and **28** compromised affinity. Encouraged by the remarkable results observed for **24** and **25**, we tested analogues with the vinyl replaced by a hydroxymethyl group. In both cases (**31** and **32**), this

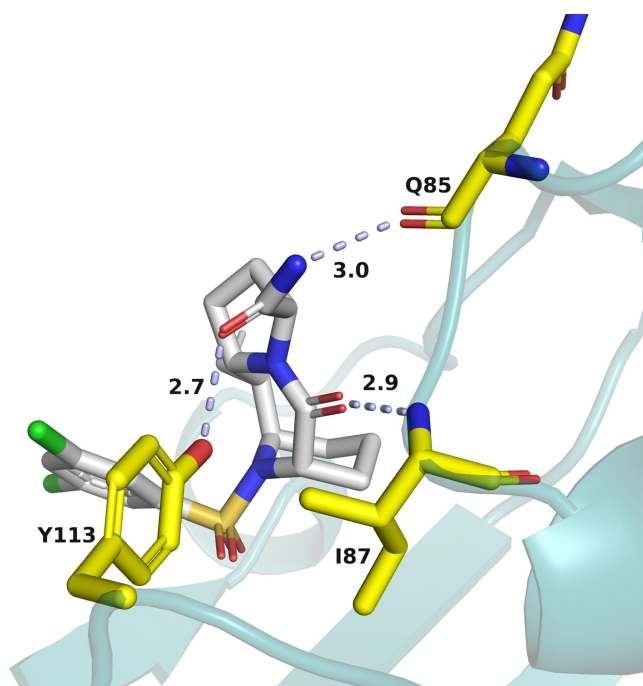


**Figure 3.** The cocrystal structure (PDB: 9EY4) of compound 21 (grey sticks) in complex with FKBP51 (cyan cartoon, key residues shown as yellow sticks). Hydrogen bonds between 21 and the protein are indicated by dotted lines with the distances in Angstrom.

modification increased affinity even more, resulting in low picomolar inhibitors for FKBP12 and sub-nanomolar ligands for FKBP51. These compounds, together with 20, were tested in a nanoBRET assay in order to determine target engagement of FKBP12 or FKBP51 in HEK293T cells<sup>[32]</sup> (Table 2). The absence of a negative charge in the case of ester 20 enhances cell potency, indicating poor permeability of carboxyl-containing compound 3. Significantly, compounds 31 and 32 both displaced the FKBP51 tracer at low nanomolar potencies, and compound 32 even attained sub-nanomolar potency for FKBP12. Taken together, this represents an almost 1000-fold improvement in biochemical as well as cellular activity compared to starting tricycle 3.

## Conclusions

In this study we developed a reliable enantioselective synthesis of a novel conformationally constrained tricyclic scaffold that was enabled by a range of synthetic transformations incl. anodic oxidation,  $\text{BF}_3$  promoted stereoselective addition of organocopper reagent and TMS-facilitated *N*-acyl iminium cyclization. Access to the tricyclic compound 3 in gram scale was crucial to allow the structure-activity relationship analysis that eventually led to compounds 31 and 32, which represent the most potent FKBP ligands known today. The cocrystal structures revealed the key interactions and uncovered subtle tricycle-specific rearrangements of the carboxyl and carboxamide substituent as well as a new hydrogen bond for the latter. The ultrahigh affinity is likely generated by precisely locking of

Entry	Structure	nanoBRET FKBP51 IC50 [nM]	nanoBRET FKBP12 IC50 [nM]
3		> 10000	1337 ± 153
20		620 ± 71	11 ± 1.4
31		8.5 ± 0.6	3.9 ± 0.3
32		3.3 ± 0.3	0.49 ± 0.04

all atoms of 31 and 32 in a conformation that is ideally preorganized for interaction with the shallow binding pocket of FKBP. The precursor series represented by bicycles 1 and 2 featured a methyl group that increase affinity by displacing a conserved but high-energy “unhappy” water molecules at the protein-ligand interface. We hypothesise that this conserved water molecule is also partially displaced by the pyrrolidine ring of the tricyclic compounds presented here, which likely contributed to the enhanced affinity. In summary, tricyclic sulfonamides represent a highly optimized scaffold for the robust generation of ultrahigh affinity FKBP ligands, e.g. as a basis for novel molecular glues. More generally, our results highlight the power of molecular complexity and modern organic chemistry to generate binding energy in a highly ligand-efficient manner.

## Supporting Information Summary

All synthetic and experimental details, as well as  $^1\text{H}$  and  $^{13}\text{C}$  NMR spectra are provided in the Supporting Information. The authors have cited additional references within the Supporting Information.<sup>[33–51]</sup>

## Acknowledgements

We would like to thank the staff of the ESRF and EMBL Grenoble for assistance and support in using beamline ID23-1 under

proposal number MX-2555. This work was supported by the BMBF grants iGLUE (03ZU1109EB) and iMIP (16GW0211K), and the LOEWE exploration grant PaaP. The raw data for pdb 9EY3 and 9EY4 can be accessed at doi:10.15151/ESRF-DC-1602472053. Open Access funding enabled and organized by Projekt DEAL.

## Conflict of Interests

The authors declare no conflict of interest.

## Data Availability Statement

The data that support the findings of this study are available in the supplementary material of this article.

**Keywords:** Rigidification · Structure-based drug design · Prolines · Fused ring systems · FK506-binding proteins

- [1] O. O. Grygorenko, D. M. Volochnyuk, B. V. Vashchenko, *Eur. J. Org. Chem.* **2021**, 2021, 6478–6510.
- [2] F. Lovering, J. Bikker, C. Humblet, *J. Med. Chem.* **2009**, *52*, 6752–6756.
- [3] For recent examples of synthesis and application of sp<sup>3</sup>-enriched building blocks see: a) J. M. Anderson, N. D. Measom, J. A. Murphy, D. L. Poole, *Angew. Chem. Int. Ed.* **2021**, *60*, 24754–24769; b) D. Dibchak, M. Snisarenko, A. Mishuk, O. Shablykin, L. Bortnichuk, O. Klymenko-Ulianov, Y. Kheylilik, I. V. Sadkova, H. S. Rzepa, P. K. Mykhailiuk, *Angew. Chem. Int. Ed.* **2023**, *62*, e202304246; c) A. Denisenko, P. Garbuz, N. M. Voloshchuk, Y. Holota, G. Al-Maali, P. Borysko, P. K. Mykhailiuk, *Nat. Chem.* **2023**, *15*, 1155–1163; d) A. Denisenko, P. Garbuz, Y. Makovetska, O. Shablykin, D. Lesyk, G. Al-Maali, R. Korzh, I. V. Sadkova, P. K. Mykhailiuk, *Chem. Sci.* **2023**, *14*, 14092–14099; e) S. L. Degorce, M. S. Bodnarchuk, I. A. Cumming, J. S. Scott, *J. Med. Chem.* **2018**, *61*, 8934–8943.
- [4] C. Borsari, D. Rageot, A. Dall'Asen, T. Bohnacker, A. Melone, A. M. Sele, E. Jackson, J.-B. Langlois, F. Beauflis, P. Hebeisen, D. Fabbro, P. Hillmann, M. P. Wymann, *J. Med. Chem.* **2019**, *62*, 8609–8630.
- [5] A. Assadieskandar, C. Yu, P. M. Maisonneuve, I. Kurinov, F. Sicheri, C. Zhang, *ACS Med. Chem. Lett.* **2019**, *10*, 1074–1080.
- [6] D. Semenyi, M. Toutitou, C. M. Ribeiro, F. R. Pavan, L. Pisano, V. Singh, K. Chibale, G. Bano, A. Toscani, F. Manetti, B. Gianibbi, D. Castagnolo, *ACS Med. Chem. Lett.* **2022**, *13*, 63–69.
- [7] Z. Fang, Y. Song, P. Zhan, Q. Zhang, X. Liu, *Future Med. Chem.* **2014**, *6*, 885–901.
- [8] S. Gaali, R. Gopalakrishnan, Y. Wang, C. Kozany, F. Hausch, *Curr. Med. Chem.* **2011**, *18*, 5355–5379.
- [9] a) C. M. Noddings, J. L. Johnson, D. A. Agard, *Nat. Struct. Mol. Biol.* **2023**, *30*, 1867–1877; b) A. Baischew, S. Engel, M. C. Taubert, T. M. Geiger, F. Hausch, *Nat. Struct. Mol. Biol.* **2023**, *30*, 1857–1866.
- [10] A. Hähle, S. Merz, C. Meyners, F. Hausch, *Biomolecules* **2019**, *9*, 35.
- [11] V. Buffa, F. H. Knaup, T. Heymann, M. Springer, M. V. Schmidt, F. Hausch, *ACS Pharmacol. Transl. Sci.* **2023**, *6*, 361–371.
- [12] Y. Wang, A. Kirschner, A.-K. Fabian, R. Gopalakrishnan, C. Kress, B. Hoogeland, U. Koch, C. Kozany, A. Bracher, F. Hausch, *J. Med. Chem.* **2013**, *56*, 3922–3935.
- [13] R. Gopalakrishnan, C. Kozany, Y. Wang, S. Schneider, B. Hoogeland, A. Bracher, F. Hausch, *J. Med. Chem.* **2012**, *55*, 4123–4131.
- [14] M. Bischoff, C. Sippel, A. Bracher, F. Hausch, *Org. Lett.* **2014**, *16*, 5254–5257.
- [15] S. Pomplun, Y. Wang, A. Kirschner, C. Kozany, A. Bracher, F. Hausch, *Angew. Chem. Int. Ed.* **2015**, *54*, 345–348.
- [16] P. L. Purder, C. Meyners, W. O. Sugiarto, J. Kolos, F. Löhr, J. Gebel, T. Nehls, V. Dötsch, F. Lermyte, F. Hausch, *JACS Au* **2023**, *3*, 2478–2486.
- [17] T. M. Geiger, M. Walz, C. Meyners, A. Kuehn, J. K. Dreizler, W. O. Sugiarto, E. V. S. Maciel, M. Zheng, F. Lermyte, F. Hausch, *Angew. Chem. Int. Ed.* **2024**, *63*, e202309706.
- [18] R. C. Deutscher, C. Meyners, S. C. Schäfer, M. L. Repity, W. O. Sugiarto, J. Kolos, T. Heymann, T. M. Geiger, S. Knapp, F. Hausch, *ChemRxiv preprint* **2023**, DOI: 10.26434/chemrxiv-2023-4vb0m.
- [19] S. Pomplun, C. Sippel, A. Hähle, D. Tay, K. Shima, A. Klages, C. M. Ünal, B. Rieß, H. T. Toh, G. Hansen, H. S. Yoon, A. Bracher, P. Preiser, J. Rupp, M. Steinert, F. Hausch, *J. Med. Chem.* **2018**, *61*, 3660–3673.
- [20] R. C. E. Deutscher, M. Safa Karagöz, P. L. Purder, J. M. Kolos, C. Meyners, W. Oki Sugiarto, P. Krajczyk, F. Tebbe, T. M. Geiger, C. Ünal, U. A. Hellmich, M. Steinert, F. Hausch, *ChemBioChem* **2023**, *24*, e202300442.
- [21] J. M. Kolos, S. Pomplun, S. Jung, B. Rieß, P. L. Purder, A. M. Voll, S. Merz, M. Gnatzy, T. M. Geiger, I. Quist-Løkken, J. Jatzlau, P. Knaus, T. Holien, A. Bracher, C. Meyners, P. Czodrowski, V. Krewald, F. Hausch, *Chem. Sci.* **2021**, *12*, 14758–14765.
- [22] M. Bischoff, P. Mayer, C. Meyners, F. Hausch, *Chem. Eur. J.* **2020**, *26*, 4677–4681.
- [23] J. Zhong, Z. Guan, Y.-H. He, *Catal. Commun.* **2013**, *32*, 18–22.
- [24] a) C. Reuter, R. Opitz, A. Soicke, S. Dohmen, M. Barone, S. Chiha, M. T. Klein, J.-M. Neudörfl, R. Kühne, H.-G. Schmalz, *Chem. Eur. J.* **2015**, *21*, 8464–8470; b) C. Reuter, P. Huy, J.-M. Neudörfl, R. Kühne, H.-G. Schmalz, *Chem. Eur. J.* **2011**, *17*, 12037–12044; c) T. Shono, *Tetrahedron* **1984**, *40*, 811–850; d) T. Shono, H. Hamaguchi, Y. Matsumura, *J. Am. Chem. Soc.* **1975**, *97*, 4264–4268.
- [25] a) Y. Tong, Y. M. Fobian, M. Wu, N. D. Boyd, K. D. Moeller, *J. Org. Chem.* **2000**, *65*, 2484–2493; b) M. Thaning, L.-G. Wistrand, Y. Stenström, H. Lund, A. Z.-Q. Khan, J. Sandström, P. Krosgaard-Larsen, *Acta Chem. Scand.* **1992**, *46*, 194–199; c) L.-G. Wistrand, M. Skrinjar, *Tetrahedron* **1991**, *47*, 573–582.
- [26] D. L. Nascimento, I. Reim, M. Foscatto, V. R. Jensen, D. E. Fogg, *ACS Catal.* **2020**, *10*, 11623–11633.
- [27] a) T. Wdowik, C. Samojłowicz, M. Jawiczuk, A. Zarecki, K. Grell, *Synlett* **2010**, 2010, 2931–2935; b) E. Vedrenne, H. Dupont, S. Oualef, L. Elkaim, L. Grimaud, *Synlett* **2005**, 670–672; c) A. Fürstner, K. Langemann, *J. Am. Chem. Soc.* **1997**, *119*, 9130–9136.
- [28] For selected examples of using NHP esters see: a) M. D. Palkowitz, G. Laudadio, S. Kolb, J. Choi, M. S. Oderinde, T. E.-H. Ewing, P. N. Bolduc, T. Chen, H. Zhang, P. T. W. Cheng, B. Zhang, M. D. Mandler, V. D. Blaszczak, J. M. Richter, M. R. Collins, R. L. Schioldager, M. Bravo, T. G. M. Dhar, B. Vokits, Y. Zhu, P.-G. Echeverria, M. A. Poss, S. A. Shaw, S. Clementson, N. N. Petersen, P. K. Mykhailiuk, P. S. Baran, *J. Am. Chem. Soc.* **2022**, *144*, 17709–17720; b) T.-G. Chen, H. Zhang, P. K. Mykhailiuk, R. R. Merchant, C. A. Smith, T. Qin, P. S. Baran, *Angew. Chem. Int. Ed.* **2019**, *58*, 2454–2458; c) D. C. Salgueiro, B. K. Chi, I. A. Guzei, P. Garcia-Reynaga, D. J. Weix, *Angew. Chem. Int. Ed.* **2022**, *61*, e202205673; d) J. Cornella, J. T. Edwards, T. Qin, S. Kawamura, J. Wang, C.-M. Pan, R. Gianatassio, M. Schmidt, M. D. Eastgate, P. S. Baran, *J. Am. Chem. Soc.* **2016**, *138*, 2174–2177.
- [29] K. M. M. Huihui, J. A. Caputo, Z. Melchor, A. M. Olivares, A. M. Spiewak, K. A. Johnson, T. A. DiBenedetto, S. Kim, L. K. G. Ackerman, D. J. Weix, *J. Am. Chem. Soc.* **2016**, *138*, 5016–5019.
- [30] M. S. West, A. L. Gabbey, M. P. Huestis, S. A. L. Rousseaux, *Org. Lett.* **2022**, *24*, 8441–8446.
- [31] C. Kozany, A. März, C. Kress, F. Hausch, *ChemBioChem* **2009**, *10*, 1402–1410.
- [32] M. T. Gnatzy, T. M. Geiger, A. Kuehn, N. Gutfreund, M. Walz, J. M. Kolos, F. Hausch, *ChemBioChem* **2021**, *22*, 2257–2261.
- [33] J. Gabadinho, A. Beteva, M. Guijarro, V. Rey-Bakaikoa, D. Spruce, M. W. Bowler, S. Brockhauser, D. Flot, E. J. Gordon, D. R. Hall, B. Lavault, A. A. McCarthy, J. McCarthy, E. Mitchell, S. Monaco, C. Mueller-Vieckmann, D. Nurizzo, R. B. G. Ravelli, X. Thibault, M. A. Walsh, G. A. Leonard, S. M. McSweeney, *J. Synchrotron Radiat.* **2010**, *17*, 700–707.
- [34] E. Potterton, P. Briggs, M. Turkenburg, E. Dodson, *Acta Crystallogr. D Biol. Crystallogr.* **2003**, *59*, 1131–1137.
- [35] M. D. Winn, C. C. Ballard, K. D. Cowtan, E. J. Dodson, P. Emsley, P. R. Evans, R. M. Keegan, E. B. Krissinel, A. G. W. Leslie, A. McCoy, S. J. McNicholas, G. N. Murshudov, N. S. Pannu, E. A. Potterton, H. R. Powell, R. J. Read, A. Vagin, K. S. Wilson, *Acta Crystallogr. D Biol. Crystallogr.* **2011**, *67*, 235–242.
- [36] L. Potterton, J. Agirre, C. Ballard, K. Cowtan, E. Dodson, P. R. Evans, H. T. Jenkins, R. Keegan, E. Krissinel, K. Stevenson, A. Lebedev, S. J. McNicholas, R. A. Nicholls, M. Noble, N. S. Pannu, C. Roth, G. Sheldrick, P. Skubak, J. Turkenburg, V. Uski, F. von Delft, D. Waterman, K. Wilson, M. Winn, M. Wojdyr, *Acta Crystallogr. D Struct. Biol.* **2018**, *74*, 68–84.
- [37] G. Winter, D. G. Waterman, J. M. Parkhurst, A. S. Brewster, R. J. Gildea, M. Gerstel, L. Fuentes-Montero, M. Vollmar, T. Michels-Clark, I. D. Young, N. K. Sauter, G. Evans, *Acta Crystallogr. D Struct. Biol.* **2018**, *74*, 85–97.

- [38] Collaborative Computational Project, Number 4, *Acta Crystallogr. D Biol. Crystallogr.* **1994**, *50*, 760–763.
- [39] P. R. Evans, *Acta Crystallogr. D Biol. Crystallogr.* **2011**, *67*, 282–292.
- [40] P. R. Evans, G. N. Murshudov, *Acta Crystallogr. D Biol. Crystallogr.* **2013**, *69*, 1204–1214.
- [41] A. J. McCoy, R. W. Grosse-Kunstleve, P. D. Adams, M. D. Winn, L. C. Storoni, R. J. Read, *J. Appl. Crystallogr.* **2007**, *40*, 658–674.
- [42] A. A. Vagin, R. A. Steiner, A. A. Lebedev, L. Potterton, S. McNicholas, F. Long, G. N. Murshudov, *Acta Crystallogr. D Biol. Crystallogr.* **2004**, *60*, 2184–2195.
- [43] P. Emsley, B. Lohkamp, W. G. Scott, K. Cowtan, *Acta Crystallogr. D Biol. Crystallogr.* **2010**, *66*, 486–501.
- [44] G. N. Murshudov, P. Skubák, A. A. Lebedev, N. S. Pannu, R. A. Steiner, R. A. Nicholls, M. D. Winn, F. Long, A. A. Vagin, *Acta Crystallogr. D Biol. Crystallogr.* **2011**, *67*, 355–367.
- [45] R. A. Nicholls, F. Long, G. N. Murshudov, *Acta Crystallogr. D Biol. Crystallogr.* **2012**, *68*, 404–417.
- [46] G. N. Murshudov, A. A. Vagin, E. J. Dodson, *Acta Crystallogr. D Biol. Crystallogr.* **1997**, *53*, 240–255.
- [47] M. D. Winn, G. N. Murshudov, M. Z. Papiz, *Methods Enzymol.* **2003**, *374*, 300–321.
- [48] F. Long, R. A. Nicholls, P. Emsley, S. Graeulis, A. Merkys, A. Vaitkus, G. N. Murshudov, *Acta Crystallogr. D Struct. Biol.* **2017**, *73*, 112–122.
- [49] R. Gawin, A. Kozakiewicz, P. A. Guńka, P. Dąbrowski, K. Skowerski, *Angew. Chem. Int. Ed.* **2017**, *56*, 981–986.
- [50] J. R. Walker, M. P. Hall, C. A. Zimprich, M. B. Robers, S. J. Duellman, T. Machleidt, J. Rodriguez, W. Zhou, *ACS Chem. Biol.* **2017**, *12*, 1028–1037.
- [51] E. P. Coutant, G. Gagnot, V. Hervin, R. Baatallah, S. Goyard, Y. Jacob, T. Rose, Y. L. Janin, *Chem. Eur. J.* **2020**, *26*, 948–958.

---

Manuscript received: April 10, 2024  
Accepted manuscript online: June 5, 2024  
Version of record online: July 25, 2024